Bull. Mater. Sci. (2021) 44:115
https://doi.org/10.1007/s12034-021-02410-9

Facile wet-chemical synthesis and evaluation of physico-chemical characteristics of novel nanocrystalline $NdCoO_3$-based perovskite oxide as cathode for LT-SOFC applications

SRINIVASAN DHARANI PRIYA[1], ARPUTHARAJ SAMSON NESARAJ[1,*] and ANBURAJ IMMANUEL SELVAKUMAR[2]

[1]Department of Applied Chemistry, Karunya Institute of Technology and Sciences (Deemed to be University), Coimbatore 641114, India

[2]Department of Electrical and Electronics Engineering, Karunya Institute of Technology and Sciences (Deemed to be University), Coimbatore 641114, India

*Author for correspondence (drsamson@karunya.edu)

MS received 4 July 2020; accepted 28 December 2020

Abstract. The material characteristics study of nanocrystalline cathode from perovskite family for low temperature solid oxide fuel cell (LT-SOFC) application was reported in this study. The nanocrystalline perovskite with composition of $Nd_{0.90}Sr_{0.10}Co_{0.90}Fe_{0.10}O_{3-\delta}$ (NSCFO) was prepared using cost-effective, simple, room temperature chemical precipitation method. The phase characterization was studied using X-ray powder diffraction analysis, which shows single fluorite cubic phase structure, wherein nanocrystallinity is retained (crystallite size 17.5 nm). The metal oxide bond was confirmed by Fourier transform infrared characterization. The surface morphology was studied using scanning electron microscopy, which exhibits distorted cubic structure with agglomerations with size of about ~300 nm, which coincides with particle size data. The elemental composition was confirmed by energy-dispersive X-ray microanalysis mapping. The electrical behaviour of NSCFO composition was studied and the Nyquist plot exhibits the conductivity of 1.37×10^{-1} S cm^{-1} at 600°C with the activation energy of 0.355 eV. The acquired physical and electrochemical characterization results were scrutinized in order to use the materials as an efficient cathode in LT-SOFC.

Keywords. $NdCoO_3$-based cathode; facile synthesis; physical and electrochemical studies; LT-SOFC.

1. Introduction

Solid oxide fuel cells (SOFCs) have fascinated lots of recognition as an electrochemical device that directly converts the chemical energy of fuel into electrical energy by virtue of their high efficiency, low emission and fuel flexibility [1]. Typical SOFC works at the temperature range of 900–1000°C [2]. The evolution of SOFC technology is limited by its high operating temperature. By reducing the operating temperature (~600°C), the efficiency of the system increases and takes the technology of SOFC to the next level. Even so, the low operating temperature leads to the stagnant kinetics of oxygen reduction reaction (ORR) at cathode, which is one of the main limitations [3]. To overcome such limitation, new cathode materials should be optimized to operate SOFC at low temperature. Among new generations of materials, perovskite structure (ABO_3) sticks out because of their all-rounder capability [4]. It is possible to develop wide range of perovskite cathode with excellent properties by optimizing the correct A- and B-site cations and inclusion of dopants. $La_{1-x}Sr_xMnO_{3-\delta}$ (LSM) [5] and $La_{1-x}Sr_xCoO_{3-\delta}$ (LSC) [6] were the typical cathode materials, which have been used widely in SOFC. The partial substitution of Sr^{2+} on La^{3+} in the A-site leads to the formation of oxygen vacancies, inducing highest electronic conductivity. The main limitation of LSM cathode is low ionic conductivity, which relates to the Mn charge compensation where oxygen vacancies are not generated. The cathode materials offering mixed ionic and electronic conductivities (MIEC) are considered as the best candidates because of their extended activity sites for ORR, when compared with purely electronic conducting [7]. A number of such materials offering MIEC cathode were reported, including $Sm_{0.5}Sr_{0.5}CoO_{3-\delta}$ (SSC) [8], $Ba_{0.5}Sr_{0.5}Co_{0.8}Fe_{0.2}O_{3-\delta}$ (BSCF) [9] and $La_{0.6}Sr_{0.4}Co_{12_x}Fe_xO_{3-\delta}$ (LSCF) [10] based perovskite cathode materials for high and intermediate temperature SOFCs. Cobaltites with general formula $RECoO_3$ (RE = rare earth like La, Nd, Gd, etc.)

Electronic supplementary material: The online version contains supplementary material available at https://doi.org/10.1007/s12034-021-02410-9.

Published online: 23 April 2021

have also been widely studied as cathodes in SOFCs [11]. Hui *et al* [12] have reported that a material with composition $Ba_{0.5}Pr_{0.5}Co_{0.8}Fe_{0.2}O_{3-\delta}$ (BPCF) perovskite oxides shows better conductivity of about 1500 S cm^{-1} at 600°C than $Sm_{0.5}Sr_{0.5}CoO_{3-\delta}$ cathode. To the best of our knowledge, few studies report the possible synergistic effects of co-doping highly charged dopants on catalysing the ORR in LT-SOFC cathodes.

In this research work, we proposed a new composition of perovskite oxide-based cathode; i.e., neodymium cobalt oxide ($NdCoO_3$) doped with strontium (Sr) and iron (Fe) ($Nd_{0.90}Sr_{0.10}Co_{0.90}Fe_{0.10}O_{3-\delta}$ referred to as NSCFO) for SOFC, which was prepared by a simple cost-effective wet-chemical method. This perovskites exhibit decent conductivity at 600°C and may show better ORR activity at low temperature. The physical and the electrochemical characteristics of the prepared cathode materials were studied systematically in order to use them as an efficient cathode for LT-SOFC application.

2. Materials and methods

2.1 *Materials*

The chemicals such as neodymium oxide (99%, SRL, India), cobalt nitrate hexahydrate (99.9%, Loba, India), strontium nitrate (99.9%, SRL, India), iron nitrate nonahydrate (99.9%, SRL), sodium hydroxide (98%, Avra, India), nitric acid (98%, Fischer, India) and ethanol (99.9%, CS, China) were used in the experiment. All the chemicals were used as such without any further purification.

2.2 *Facile chemical synthesis of NSCFO nanoparticles*

Appropriate amount of neodymium oxide is dissolved in minimal amount of concentrated nitric acid and diluted in water. The precursor solution was made by stirring 10 ml of neodymium suspension and 10 ml of cobalt nitrate solution, which was prepared by dissolving appropriate amount of cobalt nitrate salt in distilled water. Sodium hydroxide (NaOH), 10 ml, solution was added as a precipitating agent to the stoichiometric precursor solution, which resulted in dark blue coloured precipitate of neodymium and cobalt hydroxides [$Nd(OH)_3$ + $Co(OH)_2$]. To the above precipitating mixture, 10 ml of prepared strontium nitrate solution and 10 ml of prepared iron nitrate solution were added simultaneously. The entire mixture was stirred continuously at 700 rpm for 30 min at room temperature. The resulting mixture of hydroxide precipitate [$Nd(OH)_3$ + $Sr(OH)_2$ + $Co(OH)_2$ + $Fe(OH)_3$] was filtered and washed several times with water and ethanol. The obtained precipitate was dried overnight at 80°C in hot air oven. The resulting dark green coloured dried powder was finely ground in a mortar and calcined at 800°C for 3 h to get phase pure NSCFO nanoparticles. The schematic representation on preparation of obtained NSCFO powder is given in figure 1. The main reaction to prepare NSCFO nanoparticles by facile chemical precipitation route is given in equation (1):

$$0.90Nd(NO_3)_3 + 0.10Sr(NO_3)_2 + 0.90Co(NO_3)_2 + 0.10Fe(NO_3)_3 + 5NaOH \rightarrow Nd_{0.90}Sr_{0.10}Co_{0.90}Fe_{0.10}O_{3-\delta} + 5NaNO_3 + xH_2O \quad (1)$$

2.3 *Physical and electrochemical characterization of NSCFO nanoparticles*

The calcination of perovskite cathode material was done at 800°C in a high temperature furnace (model: Toshiba, India). Shimadzu XRD 6000 X-ray diffractometer using CuKα radiation was used for phase study of the calcined perovskite materials. The lattice parameter for the sample was calculated by least square fitting method, using DOS computer programming. Shimadzu IR Prestige–21 model–FTIR spectrometer was employed to record the Fourier transform infrared (FT-IR) spectra of the materials in the wavelength range of 4000–400 cm^{-1}. The particle size of the powder was measured using Malvern Particle Size Analyzer using triple distilled water as medium. The surface morphology of the particles was studied by means of JEOL Model JSM-6360 scanning electron microscope. Energy-dispersive X-ray microanalysis (EDAX) was also performed with JEOL Model JSM-6360 to find out the atomic weight percentage of elements present in the samples. The sintering behaviour of the nanocomposite pellet was studied at 800°C in a high temperature furnace (model: Toshibha, India). Complex impedance spectroscopy measurements were studied for the sintered sample using a Solatron 1260 frequency response analyzer (FRA), combined with Solatron 1296 electrochemical interface (ECI).

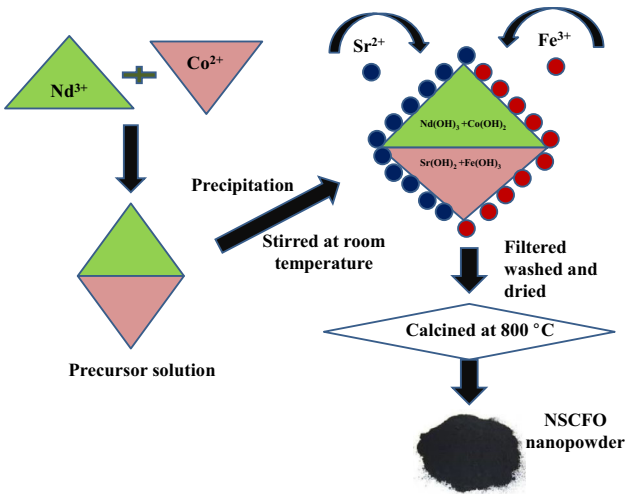

Figure 1. Schematic representation on preparation of $Nd_{0.90}Sr_{0.10}Co_{0.90}Fe_{0.10}O_{3-\delta}$ (NSCFO) by facile chemical route.

3. Results and discussion

3.1 *XRD studies*

Figure 2 exhibits the X-ray diffraction (XRD) pattern of $Nd_{0.90}Sr_{0.10}Co_{0.90}Fe_{0.10}O_{3-\delta}$ (NSCFO) nanopowder prepared by simple wet-chemical precipitation method. The observed XRD peaks were compared with the standard JCPDS data of $NdCoO_3$ powders (JCPDS No. 25-1064). The peaks observed at 23.585, 26.570, 33.532, 35.615, 40.003, 41.415, 48.123, 54.000, 55.828, 59.834, 59.824, 61.514, 66.736, 70.000, 71.800, 76.281 and 77.393 could be indexed to the hkl planes, such as, (200), (210), (220), (300), (311), (222), (400), (410), (420), (421), (422), (430), (520), (440), (441), (600) and (610), respectively. These are the planes of face centred cubic geometry of $NdCoO_3$. The introduction of strontium and iron into formed neodymium cobalt oxide could cause only a small shift in the 2θ values. This shift indicates the incorporation of the Sr and Fe ions in neodymium cobalt oxide lattice. The intensity of the peaks is also slightly increased than that of the standard data, indicating an increase in crystallinity due to lattice distortion. The crystallite size was determined using Scherrer's formula (equation (2)):

$$D = k\lambda/\beta\cos\theta, \tag{2}$$

where 'D' is the crystallite size in nm, 'k' a numerical constant ($\sim$0.9), 'λ' the wavelength of X-rays (for Cu Kα radiation, λ = 1.5418 Å), 'β' the effective broadening taken as the full-width at half-maximum (FWHM; in radians), 'θ' the diffraction angle for the peak. The crystallite size of the NSCFO material was found to be 17 nm. The lattice constant was calculated from XRD data by DOS computer programming and was found to be 7.542 Å, slightly lower than pure ceria, showing agreement to the Vegard's rule.

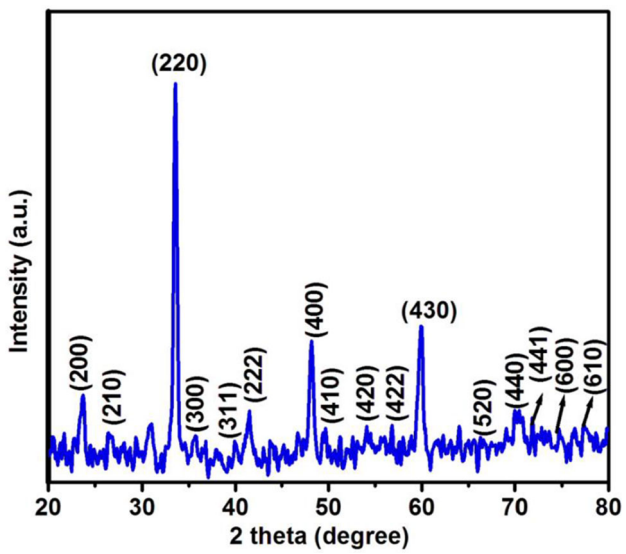

Figure 2. XRD pattern obtained on $Nd_{0.90}Sr_{0.10}Co_{0.90}Fe_{0.10}O_{3-\delta}$-based nanoparticles.

The theoretical density (D_x) values were calculated using the formula as mentioned below in equation (3):

$$D_x = (Z \times M)/(N_A \times V_{cell})\,\mathrm{g\,cm^{-3}}, \tag{3}$$

where 'Z' is the number of chemical species in the unit cell, 'M' the molecular mass of the sample (g mol^{-1}), 'N_A' is the Avogadro's number (6.022×10^{23}) and 'V_{cell}' unit cell volume ($V_{cell} = a^3$). The crystallographic parameters of $Nd_{0.90}Sr_{0.10}Co_{0.90}Fe_{0.10}O_{3-\delta}$ nanostructured materials are presented in table 1. It is reported that a cubic perovskite structure creates oxygen vacancies in the lattice and migrates freely among equivalent oxygen sites, and oxygen deficiency are beneficial for oxygen-ion conduction, which is critical for a cathode, particularly for LT-SOFC application. The former makes oxygen vacancies migrate freely among lattice-equivalent oxygen sites, while the latter facilitates ionic conduction. Li *et al* [13] reported cubic niobium and tantalum co-substituted perovskite $SrCo_{0.8}Nb_{0.1}Ta_{0.1}O_{3-\delta}$ as a cathode, which exhibits high ORR activity. It is clear that the reported composition may represent the highest reduction of oxygen in the LT-SOFC application.

3.2 *FT-IR studies*

The FT-IR spectra obtained on $Nd_{0.90}Sr_{0.10}Co_{0.90}Fe_{0.10}O_{3-\delta}$ (NSCFO) prepared by wet-chemical precipitation method is given in supplementary figure S3. A peak found at 3458.31 cm^{-1} is due to the stretching vibration of O–H correlated with the hydroxyl group in the sample. A band at 1641.52 cm^{-1} is sharp, which may be due to any carbonyl containing functional group in the samples. The peak found at 595.52 cm^{-1} is due to the stretching vibration of M–O bond in the sample [14].

3.3 *Particle size analysis*

The particle size pattern of $Nd_{0.90}Sr_{0.10}Co_{0.90}Fe_{0.10}O_{3-\delta}$ cathode material prepared by wet-chemical method using NaOH as a precipitating agent is shown in supplementary figure S4. For the particle size measurement, 0.001 g of NSCFO powder was sonicated in 30 ml triple distilled water for about 10 min and after which the sample was subjected for particle size analysis. From the particle size data, the presence of particles with $\sim$300 nm was observed, which may be due to the agglomeration effect because of the high temperature calcinations process [15].

3.4 *SEM studies*

Figure 3a, b and c represents the different magnifications of scanning electron microscope images of the $Nd_{0.90}Sr_{0.10}Co_{0.90}Fe_{0.10}O_{3-\delta}$ material prepared by wet-chemical

Table 1. Crystallographic parameters obtained on $Nd_{0.90}Sr_{0.10}Co_{0.90}Fe_{0.10}O_{3-\delta}$ nanoparticles in comparison with standard JCPDS data.

Sample	Crystal structure	Unit cell parameter (Å)	Unit cell volume (Å^3)	Crystallite size (nm)	Theoretical density (g cm^{-3})	Molecular weight
Standard XRD data for (F.C.C.) $NdCoO_3$ (JCPDS No. 25-1064)	Cubic (F.C.)	7.546	429.68	—	7.765	251.17
$Nd_{0.90}Sr_{0.10}Co_{0.90}Fe_{0.10}O_{3-\delta}$	Cubic (F.C.)	7.542	429.00	17.5	7.591	245.13

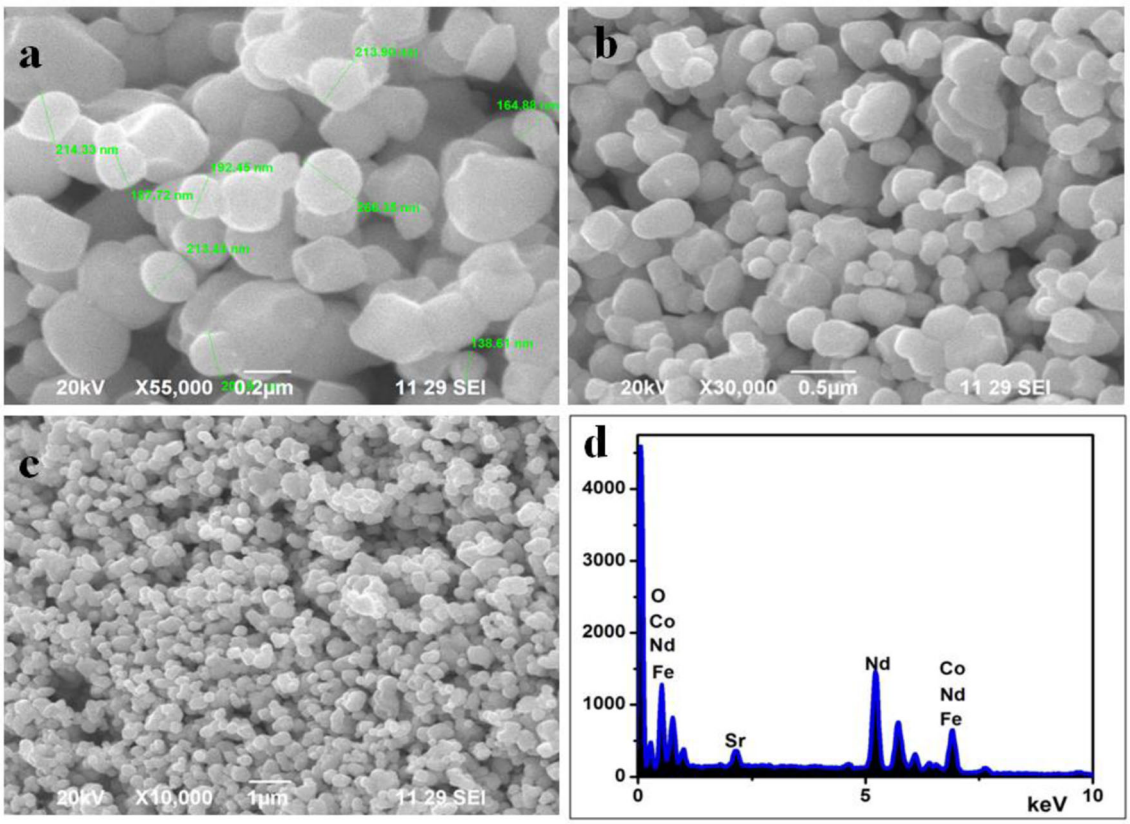

Figure 3. (**a**, **b** and **c**) SEM images obtained on $Nd_{0.90}Sr_{0.10}Co_{0.90}Fe_{0.10}O_{3-\delta}$ cathode material at different magnifications. (**d**) The energy dispersive spectra obtained on $Nd_{0.90}Sr_{0.10}Co_{0.90}Fe_{0.10}O_{3-\delta}$ cathode material.

precipitation method. The images clearly show that the grains are close-packed dense structure with agglomerated particles mostly bearing orb-like structure, having an average size of ∼300 nm coinciding particle size results. The NSCFO was calcined at 800°C for 3 h; it exhibits less agglomeration and smaller particle size and have pores [16].

3.5 *EDAX studies*

Figure 3d represents EDAX spectra of the $Nd_{0.90}Sr_{0.10}Co_{0.90}Fe_{0.10}O_{3-\delta}$ cathode material prepared by wet-chemical precipitation method. The EDAX spectra of the cathode manifest the existence of all the elements in an appropriate composition to form the desired NSCFO material. EDAX spectra of the sample NSCFO represent peaks for the elements Nd, Sr, Co, Fe and O alone. This reveals that there are no other impurity traces in the material [17]. The elemental composition data obtained on $Nd_{0.90}Sr_{0.10}Co_{0.90}Fe_{0.10}O_{3-\delta}$ by EDAX analysis are given in table 2. The measured atomic wt% of Nd, Sr, Co, Fe and O was matched well with the respective precursors used in this study. So, the co-precipitation method may be used for the preparation of $NdCoO_3$-based nanoparticles without any loss of required elements.

3.6 *Sintering characteristics*

The calcined NSCFO composition was uniaxially pressed into pellets of 1 cm in diameter and 0.176 cm thickness under the pressure of 12 MPa for about 5 min. Then, the

Table 2. Elemental composition data obtained on $Nd_{0.90}Sr_{0.10}Co_{0.90}Fe_{0.10}O_{3-\delta}$ material by EDAX analysis.

Sample	Element	Weight %	Atomic %
NSCFO cathode material	O	24.11	67.39
	Fe	2.87	2.30
	Co	16.62	12.61
	Sr	1.11	0.57
	Nd	55.29	17.14

pellet was subjected to annealing at 800°C for 8 h in air. Relative green and sintered densities were calculated geometrically (diameter and thickness were measured with a Vernier caliper and screw gauge) as an assessment of the powder compaction and sintering behaviour study. The photograph of the pellet after sintering and the surface morphology of the sintered pellet are represented in figure 4a and b. The scanning electron microscopy (SEM) image indicates that the sintered pellet consists of grains in different sizes range ($\sim$100 nm) and they present together. The surface of the pellet was found to be smooth. After sintering process, the sintered specimen was subjected to high temperature conductivity studies.

3.7 *AC impedance and conductivity studies*

The electrochemical studies for NSCFO composition was carried out in order to examine its electrical behaviour at high temperatures. The standard conditions followed to do the impedance measurements are: voltage 1.3 volts and the frequency range of 42 Hz to 5 KHz. The electrochemical impedance measurement was carried out for the sintered pellet in air atmosphere. Fitting of the measurement data was performed with the Z view software of version 3.4. The impedance data of the doped $NdCoO_3$ nanocomposite ceramic oxide pellets is fitted with the equivalent circuit ($L1 + R1(Q1/R2)$), indicated in inset of figure 5a.

The Nyquist plots of NSCFO at different temperatures (300–600°C), indicated in figure 5a, reveal that the compositions have shown a typical resistive behaviour, as there is no semicircle on the real part of the impedance (Z_{rel}) as the temperature increases. The absence of capacitance behaviour at non-blocking electrode and electrolyte interfaces is indicated by the intercept at the *Z*-real axis at lower frequencies [18]. At higher frequency when the temperature increases from 573 to 873 K, an auto-inductive element arises. It is shown in inset of figure 5a. While increasing the temperature, it is also noted that the amplitude of the semicircles corresponding to the bulk resistance decreases and disappears. A single arc is observed while the grain-boundary semicircle is slowly replaced by a tail, which may be attributed to the inductance generated due to the high electrode polarization at higher temperatures. An inductive tail is observed in the spectra above 673 K, which may be due to the inductance (L) effect generated by the electrode polarization process and the experimental setup. Ajith Kumar *et al* [18] reported $La_{0.6}Sr_{0.4}Co_{0.2}Fe_{0.8}O_{3-\delta}$–$Ce_{0.8}Sm_{0.1}Gd_{0.1}O_{1.90}$ nanocomposite cathode for intermediate temperature SOFCs. In their work, they reported more or less similar impedance spectra for their compositions (L1-G10 and L2-G20). The EIS spectra shown in figure 5a also clearly indicate that NSCFO composition has lower resistance on increasing temperature. Soltanizade *et al* [19] have reported temperature dependency of nano-catalysts on composition of $La_{0.6}Sr_{0.4}Co_{0.2}Fe_{0.8}O_{3-\delta}$ cathode. In this

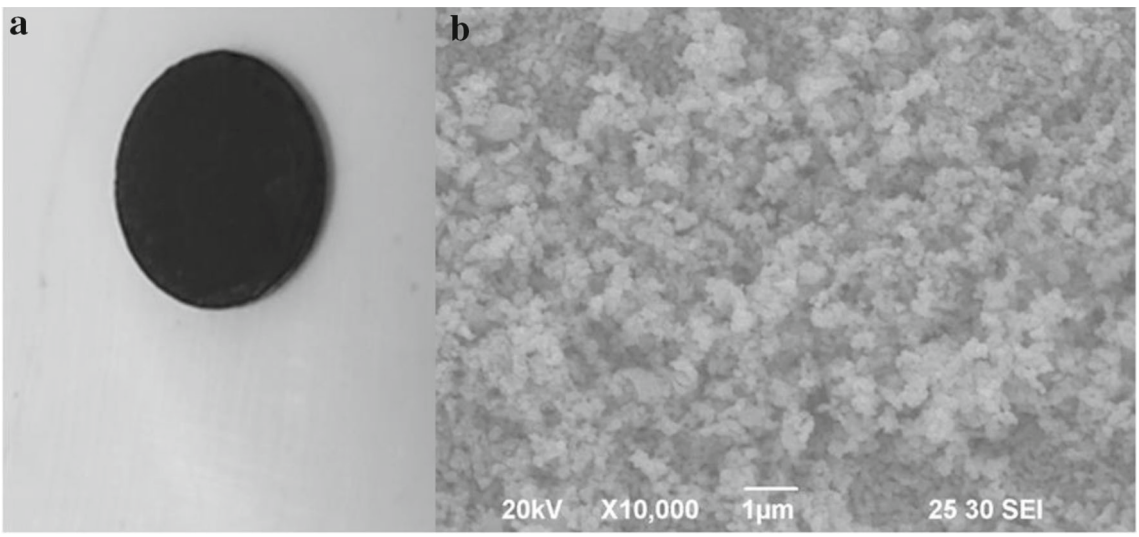

Figure 4. (**a**) Photograph of NSCFO cathode specimen sintered at 800°C for 8 h, and (**b**) SEM image of NSCFO pellet after sintering at 800°C for 8 h (magnification 10,000 times).

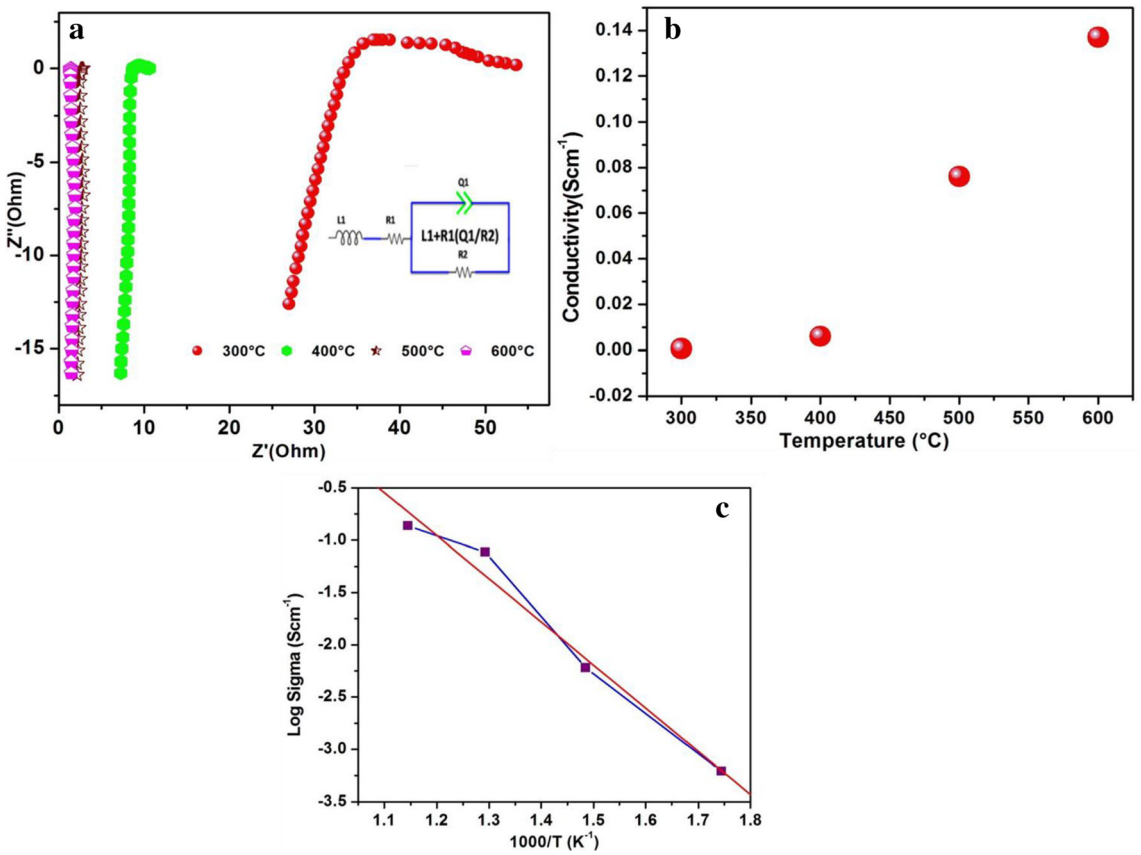

Figure 5. (**a**) Impedance spectra of NSCFO pellet at different temperatures (300–600°C). (**b**) Conductivity of NSCFO cathode specimen at different temperatures (300–600°C) and (**c**) Arrhenius plot for NSCFO cathode specimen.

work, they fitted their impedance spectra with an equivalent circuit similar to our results. The total ionic conductivity of the NSCFO material pellets has been calculated by using equation (4) and plotted as a function of temperature:

$$\sigma = \frac{1}{R} \times \frac{L}{A} \mathrm{S\,cm^{-1}} \tag{4}$$

where R is total ohmic resistance (Ω), L distance between the electrodes (thickness of the pellet in cm) and A the cross-sectional area of the sample (cm). The conductivity of the NSCFO composition at temperature is given in figure 5b. The electrical conductivity increases with increase in temperature as expected for the sample. The perovskites composition exhibits better conductivity than many of the reported materials. Zhang *et al* [20] have reported $La_{1.9}M_{0.1}Ce_2O_7$ (M = Nd, Sm, Dy, Y, In) exhibiting electrical conductivity of about 0.82×10^{-2} S cm^{-1} at air atmosphere. Tao and Irvine [21] have reported $(La_{0.75}Sr_{0.25})_{12}xCr_{0.5}Mn_{0.5}O_{3-\delta}$ cathode exhibiting electrical conductivity of about 38 S cm^{-1} in air atmosphere. Ajith Kumar *et al* [18] have reported $La_{0.6}Sr_{0.4}Co_{0.2}Fe_{0.8}O_{3-\delta}$–$Ce_{0.8}Sm_{0.1}Gd_{0.1}O_{1.90}$ composite cathode prepared by glycine nitrate combustion method with electrical conductivity of about 0.043 S cm^{-1}.

3.8 *Arrhenius plot and activation energy*

Using Arrhenius linear-fit relationship equation, the activation energies of NSCFO composition have been calculated using the equation (5), given below and presented in table 3.

$$\sigma_{dc}(T) = \sigma_o \exp(-E_a/k_B T), \tag{5}$$

'σ' is represented as direct current conductivity, T is temperature, σ_o is pre-exponential factor, E_a the activation energy and k_B is Boltzmann constant [22]. The Arrhenius plot obtained on NSCFO material is shown in figure 5c. The activation energy plays an important role to evaluate performance for oxygen diffusion and oxygen ion conductivity in electrode/cathode material. The low value of activation energy 0.355 eV emphasizes the high catalytic activity of the NSCFO electrode material. It can be seen that the equation fits the data over the temperature range studied and that the electrical conductivity increases with increasing temperature, which is characteristic from a pure MIEC. Based on the excellent physical and electrical characteristics of NSCFO, it is proposed as a novel cathode material in LTSFOC.

Table 3. Electrical characteristics of NSCFO cathode specimen.

Sample	Temperature (°C)	1000/*T*	log σ (S cm^{-1})	Slope	Activation energy (eV)
NSCFO cathode specimen	300	1.744	−3.208	−4.126	0.355
	400	1.485	−2.221		
	500	1.293	−1.114		
	600	1.145	−0.806		

4. Conclusion

$Nd_{0.90}Sr_{0.10}Co_{0.90}Fe_{0.10}O_{3-\delta}$ (NSCFO)-based cathode materials were successfully prepared by facile wet-chemical synthesis method. The prepared nanoparticles were characterized using XRD, FT-IR, particle size analysis, SEM and EDAX studies. XRD confirmed the presence of cubic (F.C.) crystalline structure in the sample. Their other structural parameters were also in line with the standard $NdCoO_3$. The presence of M–O bond in the sample was confirmed by FT-IR. The light scattering particle size analysis confirmed the presence of particles in the range of 300 nm. EDAX showed the presence of appropriate at% elements in the sample. The presence of orb-like grains was confirmed by SEM analysis with grain size range of ∼100–300 nm. The SEM image shows that the sintered specimen consists of grains in different size ranges (∼100 nm) and the surface was found to be smooth. The electrical conductivity studies revealed a good conductivity of 1.37×10^{-1} S cm^{-1} at 600°C. The conductivity value of the sintered specimen increased with respect to temperature. The activation energy was found to be 0.355 eV. The reported NSCFO composition has all the sufficient properties to be used as an efficient cathode for LT-SOFC application.

Acknowledgements

We would like to thank Central Power Research Institute (Ministry of Power, Govt. of India) (Grant No. CPRI/R&D/TC/GDEC/2019, dated 06-02-2019) for financial support. ASN acknowledges the management of Karunya Institute of Technology and Sciences, for providing necessary facilities to initiate Fuel Cell research activity in the Department of Applied Chemistry.

References

[1] Pandey A 2019 *J. Miner. Met. Mater. Soc.* **71** 88
[2] Rafique M, Nawaz H, Shahid Rafique M, Bilal Tahir M, Nabi G and Khalid N R 2019 *Int. J. Energy Res.* **43** 2423
[3] Mahato N, Banerjee A, Gupta A, Omar S and Balani K 2015 *Prog. Mater. Sci.* **72** 141
[4] Kaur P and Singh K 2020 *Ceram. Int.* **46** 5521
[5] Liu Z, Liu M, Yang L and Liu M 2013 *J. Energy Chem.* **22** 555
[6] Zhao F, Peng R and Xia C 2008 *Fuel Cells Bull.* **2** 12
[7] Burnwal S K, Bharadwaj S and Kistaiah P 2016 *J. Mol. Eng. Mater.* **04** 1630001
[8] Changrong X, William R, Fanglin C and Meilin L 2002 *Solid State Ionics* **149** 11
[9] Shao Z and Haile S M 2004 *Nature* **431** 170
[10] Da Conceição L, Silva A M, Ribeiro N F P and Souza M M V M 2011 *Mater. Res. Bull.* **46** 308
[11] Baiker, Marti P E, Keusch P, Fritsch E and Reller A 1994 *J. Catal.* **146** 268
[12] Hui R, Sun C, Yick S, Decès-Petit C, Zhang X, Maric R *et al* 2010 *Electrochim. Acta* **55** 4772
[13] Li M, Zhao M and Li F 2017 *Nat. Commun.* **8** 13990
[14] Ding X, Li M, Zhao X, Ding L, Yan Y, Wang L *et al* 2020 *Sustain. Energ. Fuels*, https://doi.org/10.1039/c9se01096c
[15] Kannan K, Radhika D, Nesaraj A S, Revathi V and Sadasivuni K K 2020 *SN Appl. Sci.* **2** 1220
[16] Yamagata C and de Mello-Castanho S R H 2010 *Mater. Sci. Forum* **660–661** 971
[17] Duan C, Hook D, Chen Y, Tong J and O'Hayre R 2017 *Energy Environ. Sci.* **10** 176
[18] Ajith Kumar S, Kuppusami P and Vengatesh P 2018 *Ceram. Int.* **44** 21188
[19] Soltanizade A, Babaei A, Ataie A and Seyed V 2019 *J. Appl. Electrochem.* **49** 1113
[20] Zhang B, Zhong Z, Tu T, Kewen W and Kaiping P 2019 *J. Power Sources* **412** 631
[21] Tao S W and Irvine J T S 2004 *J. Electrochem. Soc.* **151** A252
[22] Gil V, Moure C and Tartaj J 2007 *J. Eur. Ceram. Soc.* **27** 4205